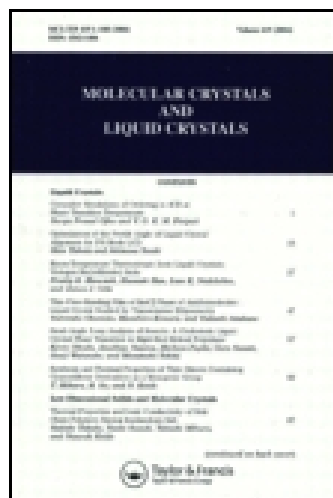


This article was downloaded by: [Michigan State University]

On: 10 February 2015, At: 11:16

Publisher: Taylor & Francis

Informa Ltd Registered in England and Wales Registered Number: 1072954 Registered office: Mortimer House, 37-41 Mortimer Street, London W1T 3JH, UK



## Molecular Crystals and Liquid Crystals

Publication details, including instructions for authors and subscription information:

<http://www.tandfonline.com/loi/gmcl18>

### Combined Tilt and Thickness Measurements on Nematic Liquid Crystal Samples

H. A. Van Sprang<sup>a</sup>

<sup>a</sup> Philips Research Laboratories, P.O. Box 80, 000 5600, JA Eindhoven, The Netherlands

Published online: 24 Sep 2006.

To cite this article: H. A. Van Sprang (1991) Combined Tilt and Thickness Measurements on Nematic Liquid Crystal Samples, *Molecular Crystals and Liquid Crystals*, 199:1, 19-26, DOI:

[10.1080/00268949108030913](https://doi.org/10.1080/00268949108030913)

To link to this article: <http://dx.doi.org/10.1080/00268949108030913>

PLEASE SCROLL DOWN FOR ARTICLE

Taylor & Francis makes every effort to ensure the accuracy of all the information (the "Content") contained in the publications on our platform. However, Taylor & Francis, our agents, and our licensors make no representations or warranties whatsoever as to the accuracy, completeness, or suitability for any purpose of the Content. Any opinions and views expressed in this publication are the opinions and views of the authors, and are not the views of or endorsed by Taylor & Francis. The accuracy of the Content should not be relied upon and should be independently verified with primary sources of information. Taylor and Francis shall not be liable for any losses, actions, claims, proceedings, demands, costs, expenses, damages, and other liabilities whatsoever or howsoever caused arising directly or indirectly in connection with, in relation to or arising out of the use of the Content.

This article may be used for research, teaching, and private study purposes. Any substantial or systematic reproduction, redistribution, reselling, loan, sub-licensing, systematic supply, or distribution in any form to anyone is expressly forbidden. Terms & Conditions of access and use can be found at <http://www.tandfonline.com/page/terms-and-conditions>

# Combined Tilt and Thickness Measurements on Nematic Liquid Crystal Samples

H. A. van SPRANG

*Phillips Research Laboratories, P.O. Box 80.000 5600 JA Eindhoven, The Netherlands*

*(Received July 25, 1990)*

A new technique is presented which enables simultaneous measurement of sample thickness and director tilt of non-twisted nematic liquid crystal cells up to about 20  $\mu\text{m}$  thick. It is shown that only  $n_o$  and  $n_e$ , the ordinary and extra ordinary refractive indices of the liquid crystal, are required with no more than three digit accuracy.

*Keywords: Nematic liquid crystals, birefringence*

It is common knowledge that on many surfaces non-zero director tilt angles can be obtained for the director of a nematic liquid crystal. In the course of time a number of experimental techniques has been developed which enable measurement of this tilt angle. Unfortunately, no such technique can be generally applied to arbitrary samples, as all of them have their own restrictions. A summary of those methods applicable to normal, flat substrate covered, test cells is presented in Table I. The only method applicable over the whole range of tilt angles is the magnetic null method.<sup>1</sup> For use with “classical” (non superconducting) magnets of about 2 T one requires samples of more than 10  $\mu\text{m}$  thickness. For studying the tilt in samples of thickness below 10  $\mu\text{m}$  we are left with either a capacitive<sup>1</sup> or an interferometric method.<sup>2,3</sup> In both methods a strong dependency is observed of the tilt angle obtained on the sample thickness.

We wanted to find a method which allows for accurate determination of tilt angles without a need to measure (in a preparatory measurement) cell thickness or capacitance of an empty cell because the sample thickness might easily change during introduction of liquid crystal.

The method we propose is based on the crystal rotation method<sup>4,5</sup> but it is more powerful due to the fact that we measure the optical phase shift instead of the transmission as a function of the rotation angle. In Figure 1 a block diagram is shown of the experimental set up. The liquid crystal sample is manufactured in such a way that no twist, splay or bend are present. It can be rotated around an axis parallel to the substrates. The director is in a plane perpendicular to the rotation axis of the sample.

The incident linear polarized light is in general elliptically polarized upon exit

TABLE I  
Comparison of methods to measure tilt angles

Method	Accessible Range $\theta$ (°)	Accuracy $\theta$ (°)	Required		References	Remarks
			Quantities	$d$ (μm)		
Magneto optic null method	0–90	0.1	—	>10	1	Only for non-twisted samples
Capacitive	0–90	0.1	$C_0, \epsilon_{  }, \epsilon_{\perp}$	—	1	Requires $C_0$ meas. on empty cell; suited for twisted samples
Interferometry	15–75	0.5	$d, n_e, n_0$	—	2, 3	Requires $d$ to be constant before and after filling
Crystal rotation	0–13 77–90	0.2	$n_e, n_0$	>10	4, 5	$\theta < 9^\circ$ in twisted structures
Conoscopy	0–17 73–90	0.2	$n_e, n_0$	>20	6	

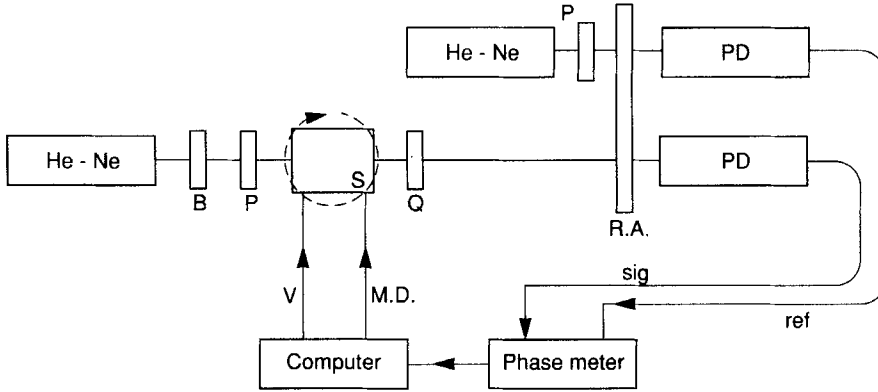


FIGURE 1 Block diagram of the experimental set-up. He-Ne indicates a He-Ne laser, B a Beam expander, P a fixed polarizer, Q a quarter waveplate, RA a rotating analyser and PD a photodetector. The rotation of the sample (Motor Drive M.D.) and the applied voltage  $V$  are controlled by a Micro computer.

from the sample. The quarter wave plate transforms it into linear polarized light with a rotation of the plane of polarization equal to  $\delta$ . This value is then measured using a rotating analyser as described before in Reference 7.

The expression for the phase difference in terms of the angle of incidence  $\phi$  with the substrate normal and the director tilt  $\theta$  with respect to the substrate is.<sup>1</sup>

$$\delta = \frac{2\pi d}{\lambda} \left[ \frac{n_0^2 - n_e^2}{n^2} \sin \theta \cos \theta \sin \phi + \frac{n_0 n_e}{n^2} \sqrt{n^2 - \sin^2 \phi} - \sqrt{n_0^2 - \sin^2 \phi} \right]$$

where

$$n^2 = n_0^2 \cos^2 \theta + n_e^2 \sin^2 \theta$$

It is this equation which is used directly in our procedure. First, the phase difference  $\delta$  is measured for a scan of  $\phi$  from  $-30^\circ$  to  $30^\circ$ . The second step is a fit of these data to the above equation using  $d$  and  $\theta$  as unknown variables. This leads to an almost independent determination of  $d$  and  $\theta$  due to the fact that both variables occur in a different way in the expression for  $\delta$ . Obviously  $d$  is directly proportional to  $\delta$  and determines the position of the  $\delta$ - $\phi$  curve on an absolute scale while  $\theta$  determines the shape of the curve. As can be learnt from the expression for  $\delta$  only  $n_e$  and  $n_o$  are left as "known" parameters. We measured the relevant indices in a slightly modified Pulfrich Refractometer which has an accuracy of better than  $1 \cdot 10^{-4}$ . In Table II we present the refractive indices for ROTN 3010 around room temperature. This liquid crystal has been used in all samples presented here.

The fit of the experimental data to the theoretical formula is performed on an IBM mainframe computer using standard IMSL Fortran software. A typical example of the results is shown in Figure 2 for a  $1.91 \mu\text{m}$  thick cell with a Polyimide orienting layer.

Obviously there is a scattering of the experimental data around the fitted results, expressed as a standard deviation of 0.98. In Figure 3 we show the results for an

TABLE II  
Refractive indices for ROTN 3010 at  $\lambda = 632 \text{ nm}$

$t$ ( $^\circ\text{C}$ )	$n_e$	$n_o$
20.0	1.6391	1.4984
20.5	1.6387	1.4983
21.0	1.6384	1.4981
21.5	1.6380	1.4980
22.0	1.6376	1.4979
22.5	1.6372	1.4978
23.0	1.6369	1.4977
23.5	1.6365	1.4976
24.0	1.6361	1.4975
24.5	1.6357	1.4974
25.0	1.6354	1.4973



FIGURE 2 Phase Retardation versus rotation angle for a  $1.91 \mu\text{m}$  thick PI cell with  $\theta = 0.27^\circ$ . Measured at  $22.2^\circ\text{C}$ .

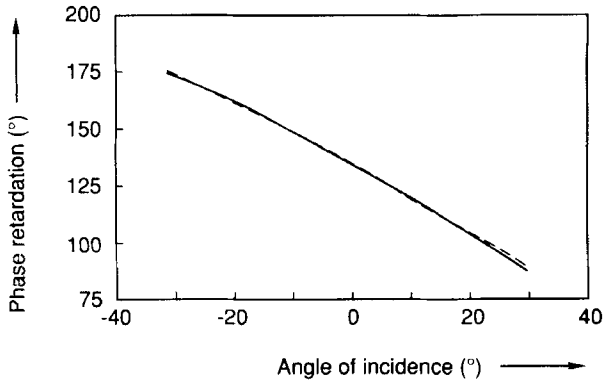


FIGURE 3 Phase Retardation v.s. rotation angle for a  $2.16 \mu\text{m}$  thick  $\text{SiO}_2$  sample with  $\theta = 25.13^\circ$ . Measured at  $25.3^\circ\text{C}$ .

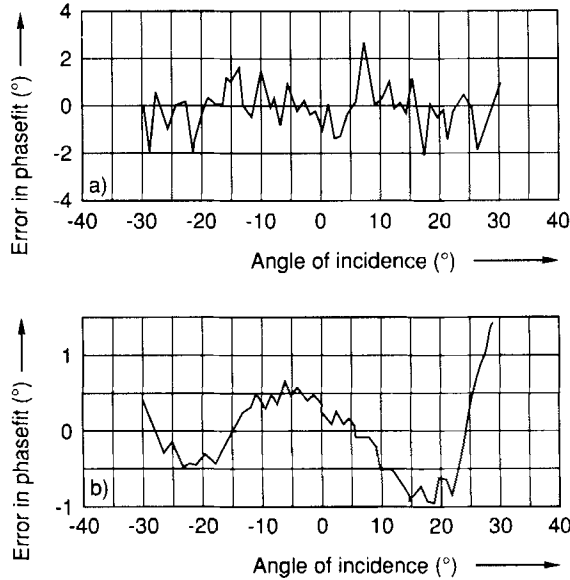


FIGURE 4 Comparison of the deviation of the fitted data from the experimental data as a function of the rotation angle: a) data for cell in Figure 2, b) data for cell in Figure 3.

evaporated  $\text{SiO}_2$  layer which had been rubbed subsequently. As can be seen the shape of the curve is different as is the observed deviation of the fit from the experimental data which amounts to a standard deviation of  $0.54^\circ$  only in Figure 3. In Figure 4 we compare the  $\text{SiO}_2$  and PI cell. Apparently in the PI cell the deviation consists of abrupt humps as a function of  $\phi$  while a gradual change is observed in Figure 4b for the  $\text{SiO}_2$  cell. To understand this difference the experimental technique must be considered in more detail. During the experiment the sample rotates over  $60^\circ$  and the laser beam (diameter  $\approx 1 \text{ mm}$ ) passes through

slightly different positions at the liquid crystal-orienting layer interface. From the photographs in Figure 5 it is immediately clear that PI is much less homogeneous at a microscopic scale than is  $\text{SiO}_2$ . Thus inhomogeneity is supposed to be the reason for the substantial noise in PI samples. Although individual differences occur, it is generally true that  $\text{SiO}_2$  cells exhibit a more gradually changing noise

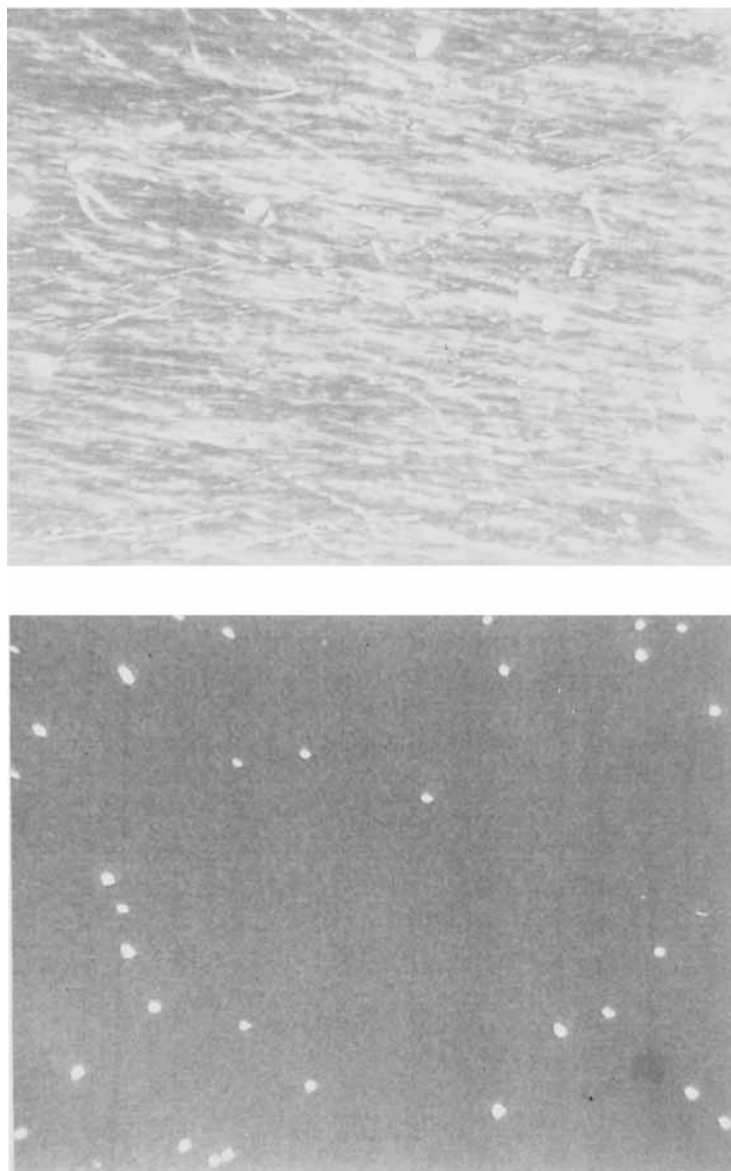


FIGURE 5 Micro photographs showing the structural difference between: a) PI oriented and b) rubbed  $\text{SiO}_2$  oriented samples. The photographs were taken under dark-field illumination and using crossed polarizers. (Magnification  $100\times$ ). See Color Plate I.

as a function of  $\phi$  than PI samples. Figures 6–8 contain further illustrations of the method.

Although the method is powerful, it also has its limitations. We can summarize them as follows:

1. For cells with  $\delta$  (632 nm) > 360°, or equivalently  $d\delta n > 1.58 \mu\text{m}$ , it is necessary to know the absolute value of  $\delta$  and not the value modulo (360°) as determined in the setup of Figure 1. For this reason we use samples supplied with ITO electrodes to which an increasing voltage up to 10V is applied. The number of times a 360° phase jump is encountered is registered by the computer and used to determine  $\delta$  at  $\phi = 0$ . For samples much thicker than 20  $\mu$  the phase jumps might occur within a too small voltage range and hence the  $\delta$  value could be wrong by 360° or more.
2. As discussed before a certain inhomogeneity might lead to a higher noise level. This does not seem to greatly influence the accuracy of the fitted results.
3. The accuracy of the refractive index data is very important to obtain accurate

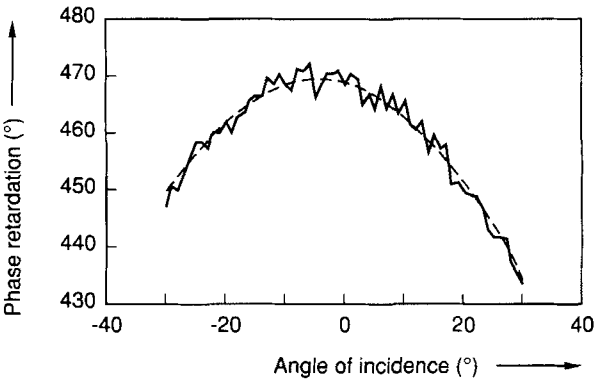


FIGURE 6 Phase retardation vs rotation angle for a 5.89  $\mu\text{m}$  thick cell with a PI orienting layer and with  $\theta = 1.33^\circ$ . Measured at 21.4°C.



FIGURE 7 Phase retardation vs rotation angle for a 61.8  $\mu\text{m}$   $\text{SiO}_2$  cell with  $\theta = 22.85^\circ$ . Measured at 25.0°C.

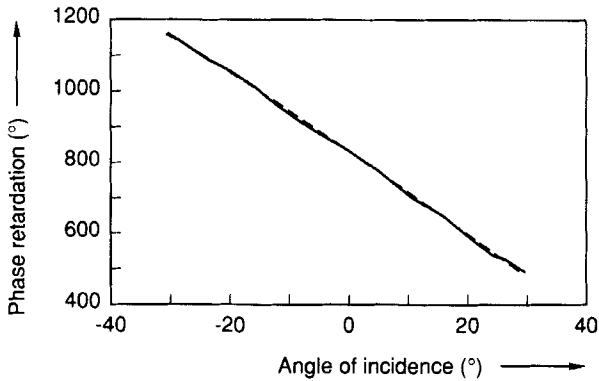


FIGURE 8 Phase Retardation vs rotation angle for a 14.59  $\mu\text{m}$   $\text{SiO}_2$  cell with  $\theta = 30.47^\circ$ . Measured at 21.4°C.

TABLE III

Influence of the variation of  $n_e$  and  $n_o$  on the obtained  $\theta$  and  $d$  values

$n_e$	$n_o$	$\theta$ (°)	$d$ ( $\mu\text{m}$ )
1.6353	1.4973	22.85	6.82
1.635	1.498	22.87	6.87
1.635	1.497	22.85	6.82
1.635	1.496	22.83	6.77
1.636	1.497	22.84	6.77
1.634	1.497	22.85	6.87
1.634	1.498	22.87	6.92
1.636	1.496	22.82	6.72
1.655	1.517	23.14	6.84

TABLE IV

Variation of  $n_e$  and  $n_o$  for a thin sample

$n_e$	$n_o$	$\theta$ (°)	$d$ ( $\mu\text{m}$ )
1.6351	1.4972	25.13	2.16
1.635	1.497	25.13	2.16
1.636	1.498	25.15	2.16
1.636	1.496	25.10	2.13
1.634	1.498	25.16	2.19

$\theta$  and  $d$  values from the fit. In Table III we show how  $n_e$  and  $n_o$  influence the results for the data of Figure 7. In general this allows for the conclusion that for values of  $n_e$  and  $n_o$  within  $1 \cdot 10^{-3}$  from their exact value an accuracy in  $\theta$  is still obtained of better than 0.1 deg while the thickness is more accurate than 0.1  $\mu\text{m}$ . From Tables IV and V similar results can be extracted for the data displayed previously in Figures 4 and 6 respectively. Thus in general the same conclusions hold independent of tilt or thickness.

Concluding we can say that the method is apparently accurate enough for appli-



TABLE V  
Variation of  $\theta$  and  $d$  with  $n_e$  and  $n_0$

$n_e$	$n_0$	$\theta$ ( $^\circ$ )	$d$ ( $\mu\text{m}$ )
1.6380	1.4980	1.33	5.89
1.637	1.499	1.33	5.98
1.639	1.497	1.32	5.81
1.64	1.50	1.33	5.89

cation to experimental samples without twist having a tilt between 0–90° degrees and a thickness up to about 20  $\mu\text{m}$ .

Inhomogeneity of the orienting layer leads to noise in the experimental data which does not significantly influence the results of the fit. The method described above yields a reliable way to determine both tilt angle and thickness in cells which are made under normal TN processing conditions but without a twisted director pattern.

References

1. T. J. Scheffer and J. Nehring, *J. Appl. Phys.*, **48**, 5 (1977) and references therein.
2. R. Simon and D. M. Nicholas, *J. Phys. D.*, **18**, 1423 (1985).
3. T. Opara, J. W. Baran and J. Zmija, *Cryst. Res. Techn.*, **23**, 1073 (1988).
4. B. B. Kosmowski, M. E. Becker and D. A. Mlynski, *Displays* April 1984, 104.
5. A. Komitow, G. Hauck and H. D. Koswig, *Cryst. Res. Techn.*, **19**, 253 (1984).
6. W. A. Crossland, J. H. Morrissy and B. Needham, *J. Phys. D.*, **9**, 2001 (1976).
7. H. A. van Sprang, *J. Physique*, **44**, 421 (1983).